Article

New Physicochemical Methodology for the Determination of the Surface Thermodynamic Properties of Solid Particles

Tayssir Hamieh [*]

Article

New Physicochemical Methodology for the Determination of the Surface Thermodynamic Properties of Solid Particles

Tayssir Hamieh [1,2]

[1] Faculty of Science and Engineering, Maastricht University, P.O. Box 616, 6200 MD Maastricht, The Netherlands, Email: t.hamieh@maastrichtuniversity.nl, Tel.: +31 6 5723 9324.

[2] Laboratory of Materials, Catalysis, Environment and Analytical Methods Laboratory (MCEMA), Faculty of Sciences, Lebanese University, Hadath, Lebanon

Abstract: The study of the surface thermodynamic properties of solid materials is primordial for the determination of the dispersive surface energy, polar enthalpy of adsorption and Lewis's acid base properties of solid particles. Inverse gas chromatography technique (IGC) at infinite dilution is the best surface technique for the determination of the surface physicochemical properties of materials. (1) Background: This paper was devoted to study the surface properties of solid materials such as alumina particles by using IGC technique. (2) Methods: Different methods and molecular models such as spherical, cylindrical, van der Waals, Redlich-Kwong, Kiselev and geometric models, were used to determine the London dispersive surface energy of solid surfaces. Hamieh model was also used and highlighted the thermal effect on the surface area of solvents. (3) Results: The variations of the dispersive surface energy and the free energy of adsorption were determined for alumina particles as a function of the temperature as well as their Lewis's acid base constants. Alumina surfaces were proved to exhibit a strong Lewis amphoteric character three time more basic than acidic (4) Conclusions: The new methodology based on Hamieh model gave the more accurate results of the physicochemical properties of the particle surfaces.

Keywords: dispersive surface energy; free energy of adsorption; enthalpy and entropy of adsoption; Lewis's acid base parameters; Hamieh thermal model; work of adhesion

1. Introduction

In most industrial processes, such as, adhesion, adsorption, polymer synthesis, dispersion, food manufacturing, pharmaceutical drugs, biomedicine, clays, composites, materials and nanomaterials, it is necessary to determine the physicochemical, surfaces and interfaces properties of solid materials. One of the most famous techniques that give information on the surface properties of materials and nanomaterials is inverse gas chromatography (IGC). This technique had a large success to determine the surface physicochemical properties of materials such as the dispersive surface energy, the specific free energy of adsorption and the Lewis-acid base parameters. Using IGC technique allowed the observation of the interactions between oxides, polymers or polymers adsorbed on oxides and organic solvent systems [1]. It was proved that this technique is very precise, sensitive, and more competitive to study the heterogeneous surfaces of solid surfaces, their physicochemical properties [2], and to determine dispersive surface energy of powdered materials [3,4]. This attractive technique was used since 1970 to quantify the specific interactions and the surface properties and glass transition of polymers, copolymers, their blends, polymer films [5-18]. It was also used to determine the surface energy, the physicochemical properties and the Lewis's acid base of metals and metal oxides, minerals, clay minerals [19-31], silicas and porous materials [32-39], nanomaterials [40-46], pharmaceuticals and food products [47-54], and other materials [55-68].

In this paper we developed a new methodology for the determination of the physicochemical, dispersive and polar properties of alumina particles by using IGC technique at infinite dilution. We used all classical IGC methods and proposed to apply the new Hamieh's thermal model [69] that was proved to be more accurate than the other models to determine the specific free enthalpy and

enthalpy of adsorption and the acid-base constants of the different materials. Eight molecular models of organic molecules were also used to calculate the dispersive component of the surface energy of solid particles.

2. Methods and Models

2.1. Classical methods

Many methods were proposed in literature and used during the last fifty years. At the beginning, Sawyer and Brookman [70] found in 1968 an excellent linearity of the logarithm of the net retention volume Vn of an adsorbed solvent on a solid, as a function of the boiling point $T_{B.P.}$ of n-alkanes $lnVn = f(T_{B.P.})$. The separation method of the dispersive (or London) and polar (or specific) interactions between a solid substrate and a polar molecule was proposed by Saint-Flour and Papirer [12,13]. These authors used the representation of $RTlnVn$ versus the logarithm of the vapor pressure P_0 of probes:

$$RTlnVn = \alpha P_0 + \beta \tag{1}$$

where R is the ideal gas constant, T the absolute temperature and α and β constants depending on the interface solid-solvent. The distance relating the representative point of $RTlnVn$ of a polar molecule to its hypothetic point located on the n-alkane straight-line determined the specific free energy of adsorption ΔG_a^{sp}. The variation of ΔG_a^{sp} versus the temperature led to the specific enthalpy ΔH_a^{sp} and entropy ΔS_a^{sp} of polar molecule adsorbed and therefore to the Lewis acid-base parameters. Five other IGC methods were proposed, to characterize the solid surfaces, a similar linearity to separate the two dispersive and polar components of the specific interactions. Two similar methods were used to determine the dispersive component γ_s^d of the surface energy of the solid. These methods are given below:

1. Dorris and Gray [71] first determined γ_s^d of solid materials by using Fowkes relation [72] and correlating the work of adhesion W_a to the free energy of adsorption ΔG_a^0 by the following relation:

$$\Delta G_a^0 = \mathcal{N} a \, W_a = 2\mathcal{N} a \sqrt{\gamma_l^d \gamma_s^d} \tag{2}$$

where a is the surface area of adsorbed molecule, γ_l^d the dispersive component of the liquid solvent γ_l^d and $\mathcal{N}$ the Avogadro's number.

Dorris and Gray introduced the increment ΔG_{-CH2-}^0 of two consecutive n-alkanes $C_nH_{2(n+1)}$ and $C_nH_{2(n+1)}$:

$$\Delta G_{-CH2-}^0 = \Delta G^0\big(C_{n+1}H_{2(n+2)}\big) - \Delta G^0\big(C_nH_{2(n+1)}\big) \tag{3}$$

By supposing the surface area of methylene group, $a_{-CH2-} = 6\text{Å}$, independent from the temperature and the surface energy γ_{-CH2-} (in mJ/m^2) of –CH2- equal to:

$$\gamma_{-CH2-} = 52.603 - 0.058 \, T \ (T \ in \ K)$$

Dorris and Gray [71] then deduced the value of γ_s^d by the equation (3):

$$\gamma_s^d = \frac{\left[RTln\left[\frac{V_n\left(C_{n+1}H_{2(n+2)}\right)}{V_n\left(C_nH_{2(n+1)}\right)} \right] \right]^2}{4\mathcal{N}^2 \, a_{-CH2-}^2 \, \gamma_{-CH2-}} \tag{4}$$

2. The method proposed by Schultz et al. [73] using Fowkes relation [72] similarly gave the free energy of adsorption ΔG_a^0 as a function of the geometric mean of the respective dispersive components of the surface energy of the liquid solvent γ_l^d and the solid γ_s^d :

$$\Delta G_a^0 = RTlnVn + C = 2\mathcal{N} a \left(\gamma_l^d \gamma_s^d\right)^{1/2} + D \tag{5}$$

where a is the surface area of probes supposed constant for all temperatures and C and D two constants depending on the used materials and the temperature. The variations of $RTlnVn$ versus $2\mathcal{N} a \left(\gamma_l^d\right)^{1/2}$ of n-alkanes and polar molecules gave both the γ_s^d and $\Delta G_a^{sp}(T)$ of the solid.

In previous studies, one determined the dispersive component of many solid materials by using the various molecular areas of Kiselev, Van der Waals (VDW), Redlich-Kwong (R-K), Kiselev, geometric, cylindrical or spherical models [74-79].

3. The method deduced from the works of Sawyer and Brookman [70] used:

$$RTlnVn = AT_{B.P.} + B \tag{6}$$

where A and B are two constants. This method gave the specific free energy and the acid base properties.

4. The method of the deformation polarizability α_0 proposed by Donnet et al. [80]. They proposed the following relation:

$$RTlnVn = E(h\nu_L)^{1/2} \alpha_{0,L} + F \qquad (7)$$

where ν_L is the electronic frequency of the probe, h the Planck's constant and E and F constants of interaction.

5. Chehimi et al. [59] used the standard enthalpy of vaporization $\Delta H_{vap.}^0$ (supposed constant) of n-alkanes and polar molecules:

$$RTlnVn = I\Delta H_{vap.}^0 + J \qquad (8)$$

where I and J are two constants. This method is similar to Saint-Flour and Papirer method using lnP_0 and that of Sawyer and Brookman using $T_{B.P.}$.

6. The method of Brendlé and Papirer [2] used the concept of the topological index χ_T that is a parameter considering the topology and the local electronic density in the polar probe structure. They gave the following relation:

$$RTlnVn = Mf(\chi_T) + N \qquad (9)$$

where M and N are two adsorption constants.

In all previous cases, the determination of $\Delta G_a^{sp}(T)$ of polar solvents versus the temperature will allow to deduce the specific enthalpy $\left(-\Delta H_a^{sp}\right)$ and entropy $\left(\Delta S_a^{sp}\right)$ of polar probes adsorbed on the solid surfaces by using equation (1):

$$\Delta G_a^{sp}(T) = \Delta H_a^{sp} - T\Delta S_a^{sp} \qquad (10)$$

Knowing of ΔH_a^{sp} polar solvents, the two respective acid base constants K_A and K_D of solids can be determined by Papirer following relation [12,13]:

$$-\Delta H^{Sp} = K_A \times DN + K_D \times AN \qquad (11)$$

That can be also written as:

$$\frac{-\Delta H^{Sp}}{AN} = K_A \frac{DN}{AN} + K_D \qquad (12)$$

where AN and DN respectively represent the electron donor and acceptor numbers of the polar molecule given by Gutmann [62] and corrected by Fowkes, K_A and K_D are the respective acid and base constant.

2.2. New methodology

2.2.1. Molecular models

The surface areas of solvents used in literature are those proposed by Kiselev and supposed constant for all temperatures. Hamieh et al [79] proposed six new molecular models that allowed the calculation of the surface areas of organic molecules: spherical (Sph.), geometric (Geom.), cylindric (Cyl.), Redlich-Kwong (R-K) and van der Waals (VDW) models compared to Kiselev results given in Table 1.

Table 1. Surface areas of n-alkanes (in Å^2) using the various molecular models.

Cn	Sph.	Geom.	R-K	Cyl.	Kiselev	VDW
C5	36.4	32.9	36.8	39.3	45	47
C6	39.6	40.7	41.3	45.5	51.5	52.7
C7	42.7	48.5	46.4	51.8	57	59.2
C8	45.7	56.2	50.8	58.1	63	64.9
C9	48.7	64	54.5	64.4	69	69.6
C10	51.7	71.8	58.2	70.7	75	74.4

All these molecular models were used for the determination of the dispersive surface energy and Lewis's acid base parameters of sold particles.

2.2.2. Hamieh's thermal model

In a recent study, Hamieh [69] proved the dependency of the surface areas of molecules on the temperature. He gave the following relation of the surface area $a(n, T)$ of n-alkanes as a function of the temperature:

$$a(n, T) = \frac{69.939\, n + 313.228}{(563.02 - T)^{1/2}} \tag{13}$$

By showing the failure of Dorris-Gray method that was largely used to determine γ_s^d of solids. This method considered the surface area a_{-CH2-} of methylene group equal to 6 Å² and constant for any used temperature. Hamieh [69] proved the non-validity of Dorris-Gray method and gave the following expression of a_{-CH2-} (in Å2) as a function of the temperature T (in K):

$$a_{-CH2-} = \frac{69.939}{(563.02 - T)^{1/2}} \tag{14}$$

Hamieh also gave the surface areas of polar molecules against the temperature by defining three new surface parameters: a first maximum temperature $T_{Max.1}$ characteristics of the interaction between the polar solvents and the PTFE fibers, a second maximum temperature $T_{Max.(X)}$, an intrinsic characteristics of the dispersive surface tension of the polar molecules and a third geometric parameter $a_{Xmin.}$ proper to the molecule X itself. The general expression of the surface area $a_X(T)$ of polar molecules was given below:

$$a_X(T) = a_{Xmin.} \times \frac{(T_{Max.1} - T)}{(563.02 - T)^{1/2}(T_{Max.(X)} - T)^{1/2}} \tag{15}$$

The large effect of the temperature on surface areas of molecules was here highlighted.

On the other hand, we highlighted an important effect of the temperature on the standard enthalpy of vaporization $\Delta H_{vap.}^0$ of organic molecules supposed constant by Chehimi et al. [59] and therefore proposed the following relation that can be used to determine the specific contribution of the Gibbs free energy of adsrption of poalr molecules on alumina particles:

$$\Delta G_a^0(T) = \delta \Delta H_{vap.}^0(T) + \varepsilon \tag{16}$$

where δ and ε are two constants of interaction.

2.2.3. The new Lewis's acid base parameters

In several cases, the Gutmann method cannot be applied because the linearity of equation 11 is not satisfied for many solid substrates. This classical relationship was corrected and a new equation was proposed by Hamieh et al. [77,81] by adding a third parameter K reflecting the amphoteric character of the oxide or polymer according to:

$$-\Delta H^{Sp} = K_A \times DN + K_D \times AN - K \times DN \times AN \tag{17}$$

By dividing by AN, we obtain:

$$\frac{-\Delta H^{Sp}}{AN} = K_A \frac{DN}{AN} + K_D - K \times DN \tag{18}$$

or:

$$X_1 = K_D + K_A X_2 - K X_3 \tag{19}$$

With:

$$X_1 = -\frac{\Delta H^{sp}}{AN},\; X_2 = \frac{DN}{AN},\; X_3 = DN \text{ and } K = K(K_A, K_D) \tag{20}$$

X_1, X_2 and X_3 are known for every polar molecule, whereas K_D, K_A and K are the unknown parameters. The problem given by equation (16) is represented by a linear system for N solvents and admits a unique solution for $N \geq 3$ giving the three unkown constants numbers: K_D, K_A and K.

On the other hand, in previous study Hamieh [83] proposed new entropic acidic ω_A and basic ω_D parameters to determine the entropic acid base character of the solid surfaces by writing:

$$\left(-\Delta S_a^{sp}\right) = \omega_A \, DN' + \omega_D \, AN' \tag{21}$$

or

$$\left(\frac{-\Delta S_a^{sp}}{AN'}\right) = \omega_A \left(\frac{DN'}{AN'}\right) + \omega_D \tag{22}$$

3. Materials and solvents

The different solid particles used in this study are furnished by Aldrich. Classical organic probes, characterized by their donor and acceptor numbers, were used in this study. Corrected acceptor number $AN' = AN\text{-}AN^d$, given by Riddle and Fowkes [82], who subtracted the contribution of Van der Waals interactions (or dispersion forces). This acceptor number was normalized by Hamieh et al. [77,81] proposed to use dimensionless donor number DN' and dimensionless acceptor number AN'. All probes (Aldrich) were highly pure grade (i.e., 99%). The probes used were n-alkanes (pentane, hexane, heptane, octane, and nonane); amphoteric solvents: acetonitrile, acetone; basic solvents: ethyl acetate, tetrahydrofuran (THF) and acidic solvent: chloroform and nitromethane.

On Table 2 gives, we gave the donor and acceptor numbers of polar probes used in this study.Chromatographic injections were made using Hamilton microsyringes. Measurements were carried out with a Focus GC Chromatograph equipped with a flame ionization detector of high sensitivity. The IGC measurements were performed on a commercial Focus GC gas chromatograph equipped with a flame ionization detector. Dried nitrogen was the carrier gas. The gas flow rate was set at 25 mL/min. The injector and detector temperatures were maintained at 400 K during the experiments.

Table 2. Normalized donor and acceptor numbers of polar molecules.

Probes	DN'	AN'	DN'/AN'	Acid base force
CCl4	0	2.3	0	acid
CHCl3	0	18.7	0	Stronger acidity
CH2Cl2	3	13.5	0.2	weaker amphoteric
Toluene	9.75	3.3	3.0	Amphoteric
Diethyl ether	48	4.9	9.8	Amphoteric
THF	50	1.9	26.3	Stronger Basicity

Chromatographic injections were made using Hamilton microsyringes. Measurements were carried out with a Focus GC Chromatograph equipped with a flame ionization detector of high sensitivity. The IGC measurements were performed on a commercial Focus GC gas chromatograph equipped with a flame ionization detector. Dried nitrogen was the carrier gas. The gas flow rate was set at 25 mL/min. The injector and detector temperatures were maintained at 400 K during the experiments.

To achieve infinite dilution, 0.1   L of each probe vapor was injected with 1   L Hamilton syringes, in order to approach linear condition gas chromatography. The column temperatures were 300 K to 460 K, varied in 20 ºC steps. Each probe injection was repeated three times, and the average retention time, t_R, was used for the calculation. The standard deviation was less than 1% in all measurements. All columns used in this study were prepared using a stainless-steel column with a 2 mm inner diameter and with an approximate length of 20 cm.

3. Results

3.1. Determination of the Gibbs free energy of adsorption

The results of the IGC technique at infinite dilution gave the net retention volume Vn of n-alkanes and polar molecules adosrbed on alumina at various temperatures in the interval [323.15K, 463.15K]. This allowed to obtain the Gibbs free energy ΔG_a^0 of adsorption by using the following fundamental thermodynamic relation of IGC:

$$\Delta G_a^0 = -\,RT \, ln \, V_n + \beta(T) \tag{23}$$

and $\beta(T)$ is given by:

$$\beta(T) = RT \, ln \left(\frac{sm\pi_0}{P_0}\right) \tag{24}$$

where s is the specific surface area of alumina and m the mass of the solid particles introduced in the coumn. Whereas, P_0 and π_0 are respectively given by the Kemball and Rideal reference state [21] at $T_0 = 0 \, ^{\circ}C$ by:

$$P_0 = 1.013 \times 10^5 \, Pa \text{ and } \pi_0 = 6.08 \times 10^{-5} \, N \, m^{-1} \tag{25}$$

The obtained results are presented in Table 3.

Table 3. Variations of the Gibbs free energy ($-\Delta G_a^0 \, in \, J \, mol^{-1}$) of adsorption of the various polar solvents on alumina particles as a function of the temperature.

T(K)	303.15	323.15	343.15	363.15	383.15	403.15	423.15	443.15	463.15
Pentane	25430	25461	25493	25609	25397	25538	25784	25651	25682
Hexane	28674	28716	28776	28827	28878	28929	29241	29032	29349
Heptane	31940	31857	31774	31692	31609	31527	31444	31361	31123
Octane	35420	35117	34813	34510	34207	33904	33601	33604	32995
Nonane	38821	38467	37716	37163	36611	36058	35506	34953	34401
CH2Cl2	61952	59637	57919	56367	54442	52966	51248	49509	47769
CHCl3	45147	42524	40448	38512	36838	34950	32911	31850	29664
CCl4	34479	34514	34449	34435	34420	34405	34391	34376	34361
THF	64519	62228	60464	58838	57449	55865	54281	53324	51507
Ether	67319	65062	63377	61763	60317	58729	56976	55555	53967
Toluene	47084	46302	45020	44028	43511	42617	41724	40831	39937

Table 3 clearly showed that the standard free energy of adsorption ($-\Delta G_a^0$) decreases for every probe when the tempertaure increases (Figure 1) and decreasing at the same time the adsorption of molecules. One also observed that the values of the free energy of adsorption of polar solvents are greater than that of n-alkanes showing the strong polar interaction between alumina and polar molecules and proving the important Lewis's acid base character of the solid surfaces.
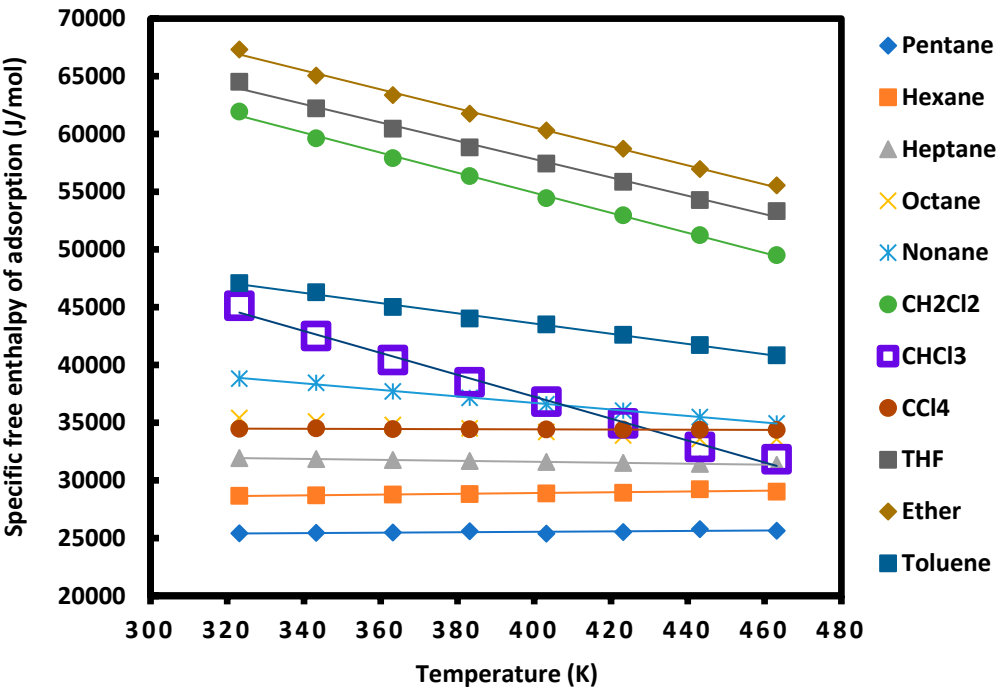
Figure 1. Variations of the surface free energy $(-\Delta G_a^0(T)$ $(in\,J/mol)$ of the solvents adsorbed on alumina particles as a function of the temperature T (K).

From Table 3 and Figure 1, one deduced the values of the standard enthalpy and entropy of adsorption for all orgnaic molecules as shown in Table 4.

Table 4. Values of standard entalpy $(-\Delta H_a^0$ $(J\,mol^{-1}))$ and entropy $(-\Delta S_a^0$ $(J\,K^{-1}\,mol^{-1}))$ of adsorption of the various organic molecules adsorbed on alumina surfaces.

Probes	$-\Delta H_a^0$	$-\Delta S_a^0$	Equation of $-\Delta G_a^0$ (T)	R²
Pentane	26284	2.2	$-\Delta G_a^0$ (T) = -2.2T + 26284	0.9967
Hexane	30423	4.5	$-\Delta G_a^0$ (T) = -4.5T + 30423	0.9967
Heptane	33192	4.1	$-\Delta G_a^0$ (T) = -4.1T + 33192	1.0000
Octane	40094	15.4	$-\Delta G_a^0$ (T) = -15.4T + 40094	0.9989
Nonane	47409	28.1	$-\Delta G_a^0$ (T) = -28.1T + 47409	0.9985
CCl4	34696	0.7	$-\Delta G_a^0$ (T) = -0.7T + 34696	0.9991
CHCl3	72931	93.8	$-\Delta G_a^0$ (T) = -93.8T + 72931	0.9949
CH2Cl2	87807	86.6	$-\Delta G_a^0$ (T) = -86.6T + 87807	0.9985
Toluene	60493	44.4	$-\Delta G_a^0$ (T) = -44.4T + 60493	0.9978
THF	86959	76.8	$-\Delta G_a^0$ (T) = -76.8T + 86959	0.9970
Ether	91555	81.5	$-\Delta G_a^0$ (T) = -81.5T + 91555	0.9976

The polar molecules on Table 4 can be classified in decreasing order of standard entalpy of adsorption:

$$\text{Diethyl ether > CH2Cl2 > THF > CHCl3 > Toluene > CCl4} \qquad (26)$$

Inequalities (21) showed that the alumina material exhibits an amphoteric character because the stronger adsorption is obtained with the amphoteric molecule such as diethyl ether.

In order to quantify the Lewis acid base properties, one used relation (10) by using the values of $(-\Delta H_a^0)$ of polar molecules. A linear relation was obtained giving

$$\frac{(-\Delta H_a^0)}{AN} = 1.112\,\frac{DN}{AN} + 3.045 \qquad (27)$$

and the values of the Lewis enthalpic acid base constants are respectively $K_A = 1.112\,kJ/mol$ and $K_D = 3.045\,kJ/mol$, whereas, those relative to the entropic constants are $\omega_A = 1.44\,J\,K^{-1}mol^{-1}$ and $\omega_D = 4.56\,J\,K^{-1}mol^{-1}$. These can be written in unitless as:

$K_A = 0.664$, $K_D = 1.820$, $\omega_A = 8.6 \times 10^{-4}$ and $\omega_D = 2.7 \times 10^{-3}$. The respective ratios of enthalpic and entropic base on acid constants are therefore given by:

$$\frac{K_D}{K_A} = 2.74 \text{ and } \frac{\omega_D}{\omega_A} = 3.2 \qquad (28)$$

These results confirmed that the alumina surfaces have an amphoteric behavior with stronger Lewis's base character 2.74 times greater than the acidic character. In this case, we proved that the Lewis and Bronsted concepts are very close showing the amphoteric behavior in both aqueous medium and solid surfaces.

3.2. London dispersive surface energy of alumina particles

In this section, we calculated the London dispersive component of alumina particles by using relations (3), (4), (12) and (13) and applying the various models of Van der Waals (VDW), Redlich-Kwong (R-K), Kiselev, geometric, cylindrical or spherical models [75-79], Dorris-Gray [69] and thermal model [71]. On Table 5, we gave the values of the London dispersive surface energy γ_s^d (T) of alumina particles as a function of the temperature for the various methods and models.
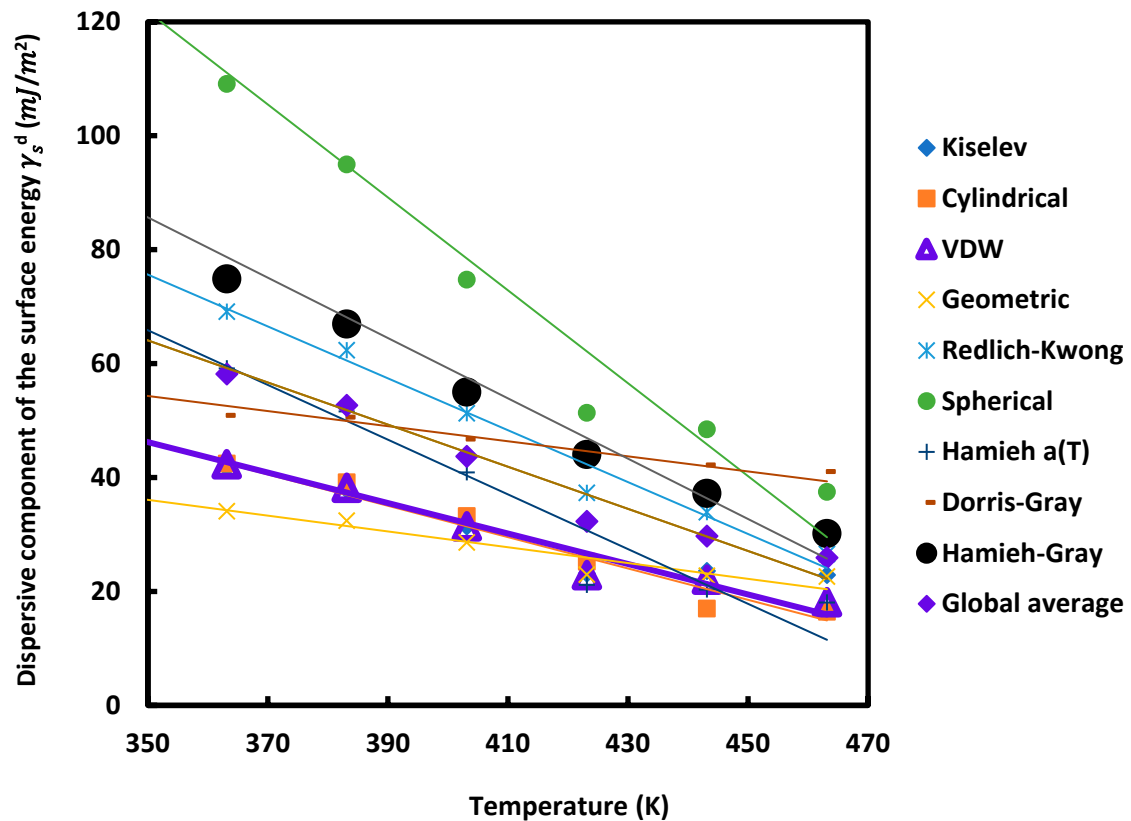
Table 5. Values of the dispersive component of the surface energy γ_s^d (mJ/m^2) of alumina particles as a function of the temperature.

γ_s^d (mJ/m^2) (alumina)

| T (K)	323.15	343.15	363.15	383.15	403.15	423.15	443.15	463.15
Kiselev	53.0	47.1	41.7	37.8	31.4	23.2	23.6	22.9
Cylindrical	52.6	47.3	42.4	39.2	33.2	25.2	17.0	16.4
VDW	54.4	48.1	42.3	38.2	31.4	22.9	22.1	18.1
Geometric	40.4	37.0	34.1	32.4	28.6	23.0	22.8	22.6
Redlich-Kwong	88.8	78.5	69.1	62.3	51.3	37.3	33.9	26.6
Spherical	148.8	127.9	109.1	95.0	74.7	51.4	48.5	37.5
Hamieh a(T)	80.6	69.3	59.2	51.6	40.9	21.2	20.4	18.1
Dorris-Gray	59.8	54.8	50.9	50.6	46.8	42.8	42.2	41.1
Hamieh-Gray	105.6	88.7	74.9	67.0	55.0	44.1	37.2	30.2
Global average	76.0	66.5	58.2	52.7	43.7	32.3	29.7	25.9

The results on Table 5 and Figure 2 showed the linear decrease of γ_s^d when the temperature increases for all applied models and methods.

Figure 2. Dispersive component of the surface energy γ_s^d (mJ/m^2) of alumina particles as a function of the temperature T (K) using different methods and models.

Three groups can be distinguished between the above models and methods:

1. The group constituted by Kiselev, cylindrical, VDW, geometric and Doris-Gray models taking into account the geometric form of n-alkanes and they presented very close values of γ_s^d and the surface of methylene group (Figure 3).
2. The second group concerns the models relative to thermal model, Redlich-Kwong equation and the global average results that concluded to the more accurate values of γ_s^d of alumina surfaces (Figure 3).
3. The third group is relative to spherical model and Gray-Hamieh model [69]. The obtained values of γ_s^d are higher than the true value, certainly because of the non-accurate values of the surface area of n-alkanes for these models (Figure 3).
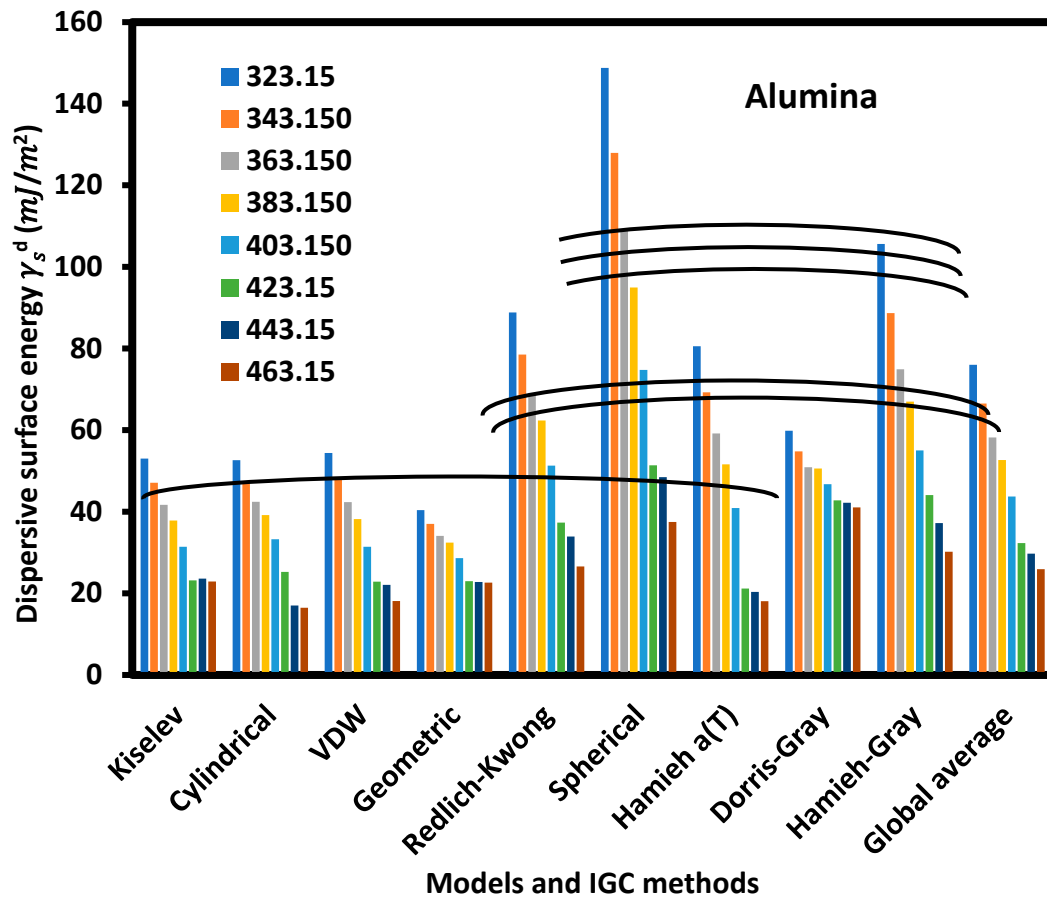
Figure 3. Dispersive surface energy γ_s^d (mJ/m^2) of alumina particles following the various methods and models for eight temperatures.

The different equations giving $\gamma_s^d(T)$ of alumina particles as a function of the temperature for the various molecular models of n-alkanes were presented on Table 6 with the values of the dispersive surface entropy ε_s^d, the extrapolated values $\gamma_s^d(T = 0K)$ and the maximum of temperature T_{Max} allowed by by the chosen molecular model. T_{Max} Was defined by the following relation:

$$T_{Max} = -\frac{\gamma_s^d(T=0K)}{\varepsilon_s^d} \qquad (29)$$

Table 6. Equations $\gamma_s^d(T)$ of alumina particles for various molecular models of n-alkanes, the dispersive surface entropy ε_s^d, the extrapolated values $\gamma_s^d(T = 0K)$ and the maximum of temperature T_{Max}.

Molecular model	$\gamma_s^d(T)$ (mJ/m²)	$\varepsilon_s^d = d\gamma_s^d/dT$ (mJ m⁻² K⁻¹)	$\gamma_s^d(T = 0K)$ (mJ/m²)	T_{Max}
Kiselev	$\gamma_s^d(T)$ = -0.232T + 126.4	-0.232	126.4	544.36
Cylindrical	$\gamma_s^d(T)$ = -0.275T + 142.3	-0.275	142.3	517.41
VDW	$\gamma_s^d(T)$ = -0.2674T + 139.8	-0.267	139.8	522.89
Geometric	$\gamma_s^d(T)$ = -0.138T + 84.6	-0.139	84.6	610.58
Redlich-Kwong	$\gamma_s^d(T)$ = -0.455T + 235.1	-0.456	235.1	516.05
Spherical	$\gamma_s^d(T)$ = -0.815T + 407.2	-0.815	407.2	499.39
Hamieh model	$\gamma_s^d(T)$ = 0.480T + 233.9	-0.480	233.9	487.21
Dorris-Gray	$\gamma_s^d(T)$ = -0.132T + 100.7	-0.133	100.7	760.08
Hamieh-Gray	$\gamma_s^d(T)$ = -0.500T + 271.0	-0.530	271.0	511.78
Global average	$\gamma_s^d(T)$ = -0.370T + 141.2	-0.370	193.4	523.42

Table 6 showed the large difference between the values of dispersive surface entropy of the different molecular models compared to that given by Hamieh thermal model ($\varepsilon_s^d = -0.480\ mJ\ m^{-2}K^{-1}$) and the highest value obtained by the spherical model. The important result obtained here is the average value of $T_{Max} = 523.42\ K$ with comparable values to the various models excepted for the case of Dorris -Gray.

3.2. Surface thermodynamic of alumina particles

3.2.1. The Gibbs specific free energy of adsorption

The variations of the Gibbs specific free energy ($\Delta G_a^{sp}(T)$) of the various polar solvents adsorbed on silica particle surface as a function of the temperature T were given on Table S1 (Supporting Information) for the various models such as Kiselev, Van der Waals, Redlich-Kwong, geometric, spherical and thermal models and IGC methods such as Boiling point, vapor pressure, deformation polarizability, enthalpy of vaporization, $\Delta H_{vap.}^0$, $\Delta H_{vap.}^0$ (T) and Topological index methods.

The values $\Delta G_a^{sp}(T)$ presented on Table S1 proved that there is no universal method that can give accurate results excepted the thermal model that took into account the temperature effect on the surface area of molecules. We observed on Table S1 the large difference in results obtained with the different models and methods that can reach 100% of the results given by the thermal model. We showed on Figure 4 the disparity in obtained results with different polar molecules adsorbed on alumina surfaces. The linear variations of $\Delta G_a^{sp}(T)$ plotted on Figure 4 and Table 7 giving the corresponding equations clearly proved that the slope and the ordinate at origin strongly depend on the chosen model or used method and for every polar molecule.
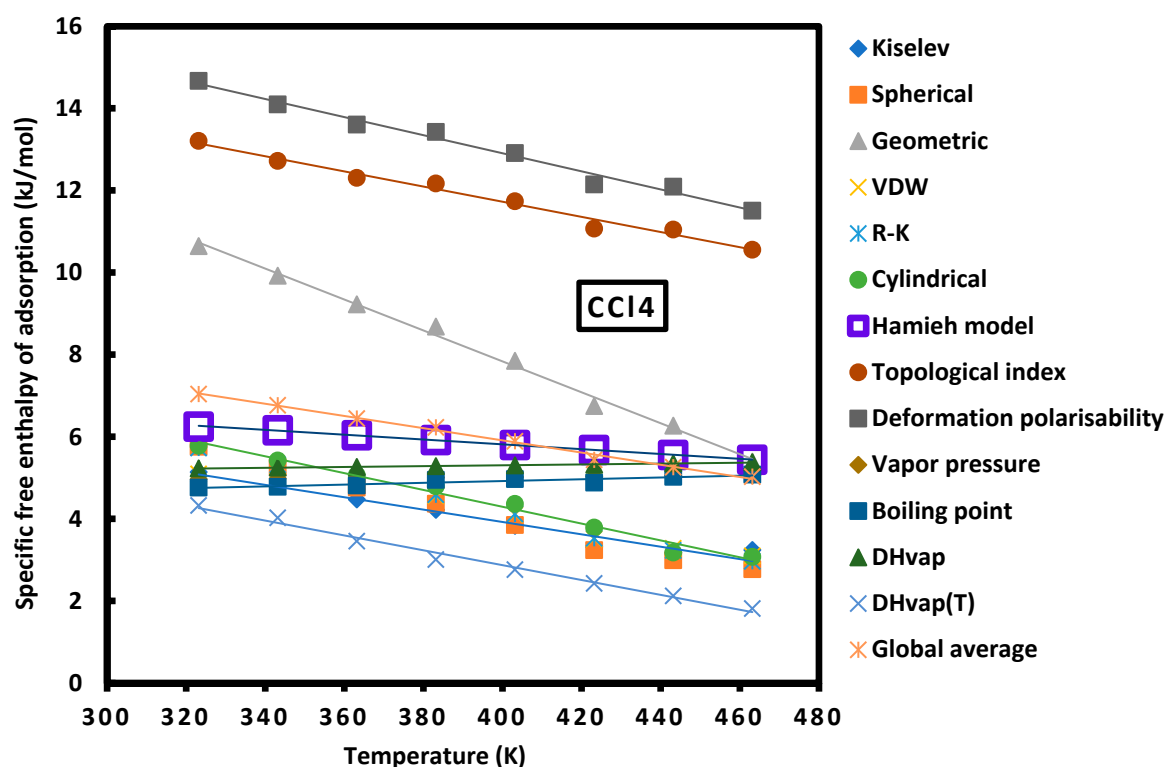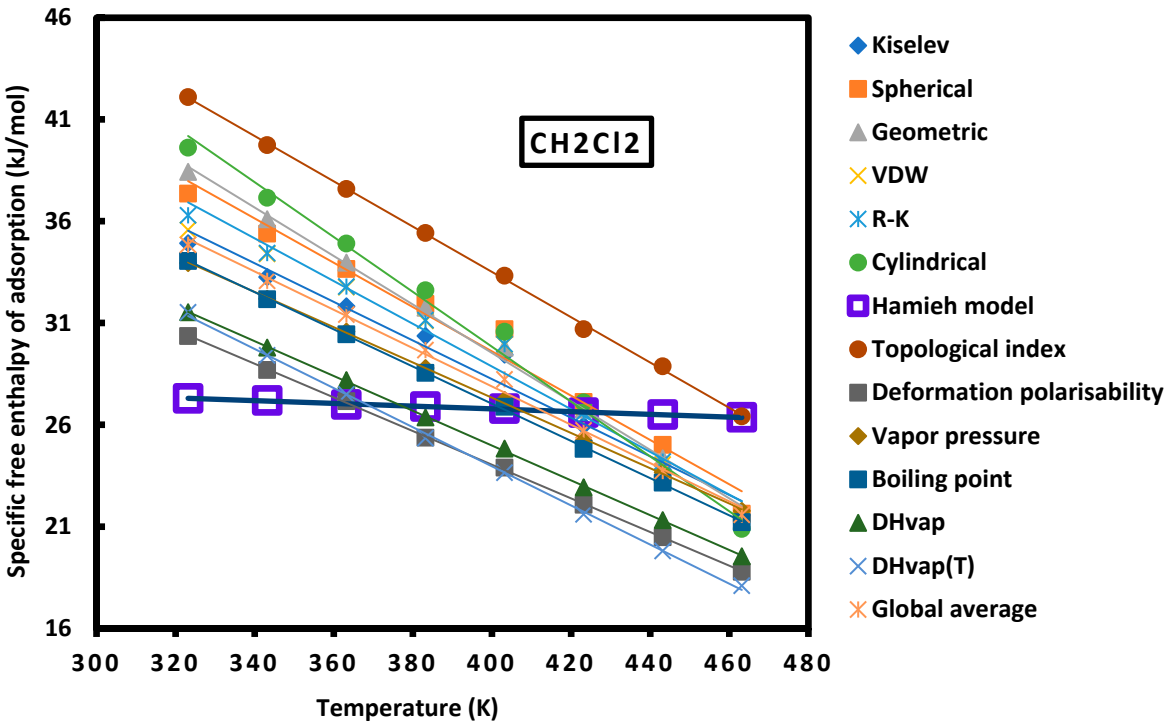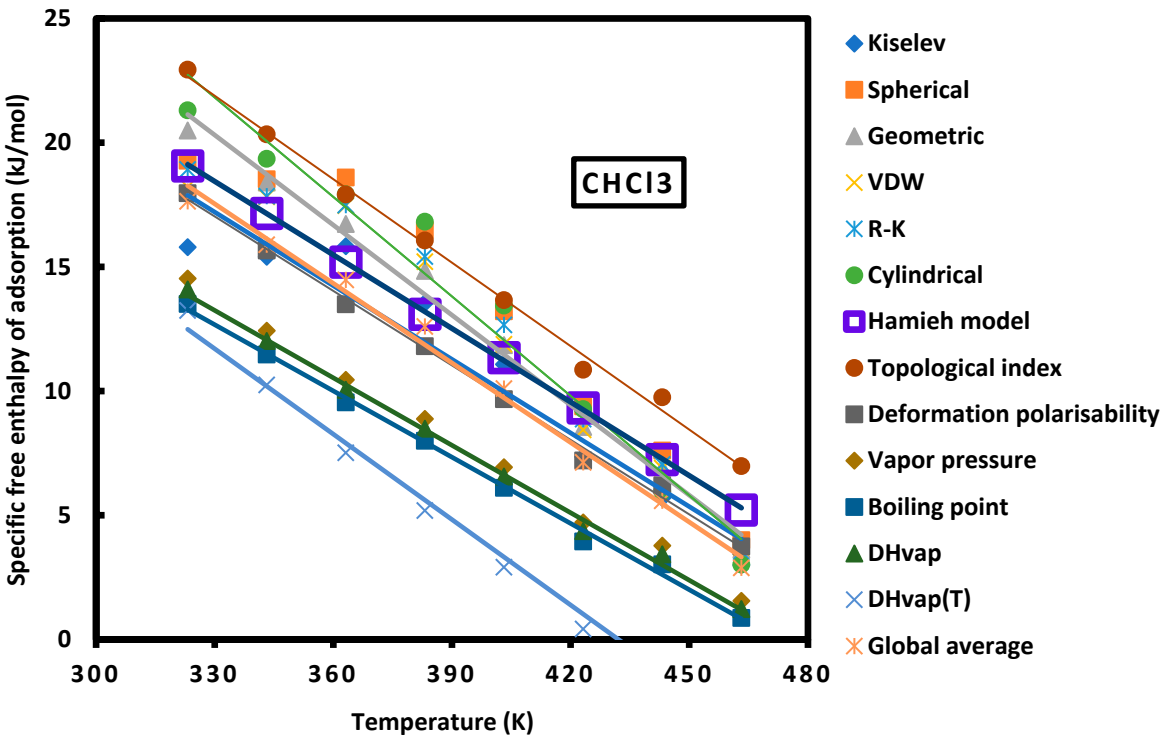

Figure 4a. CCl4.

Figure 4b. CH2Cl2.

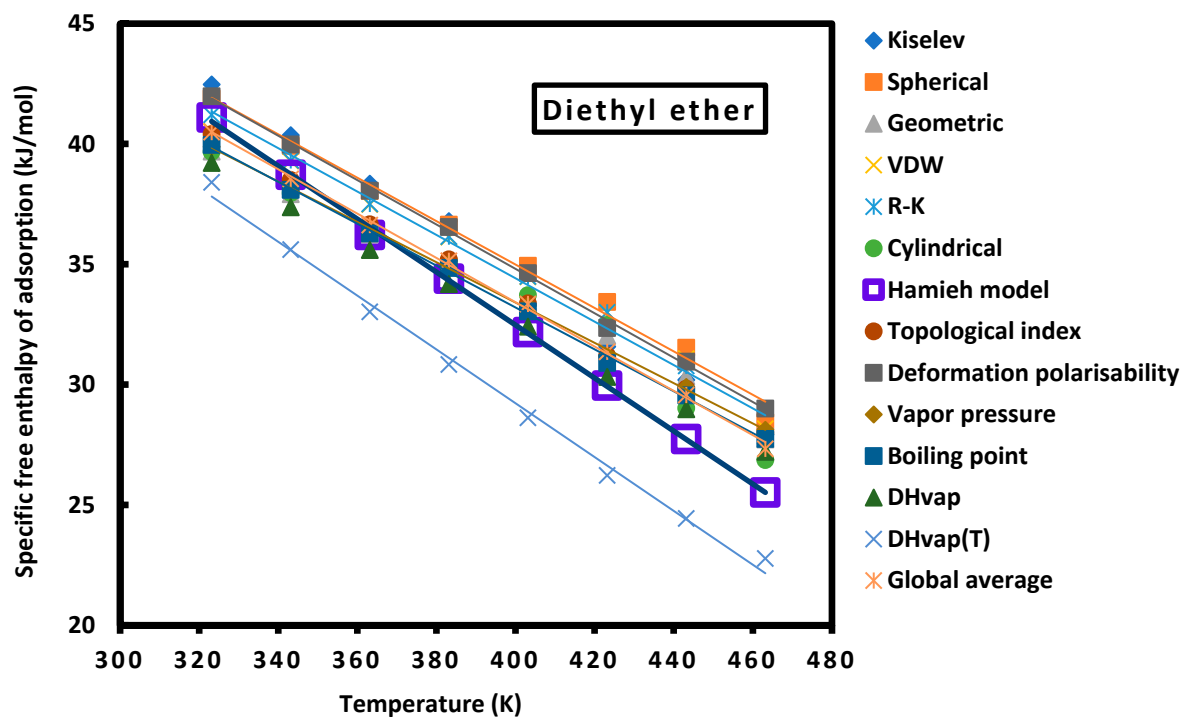**Figure 4c.** CHCl3.
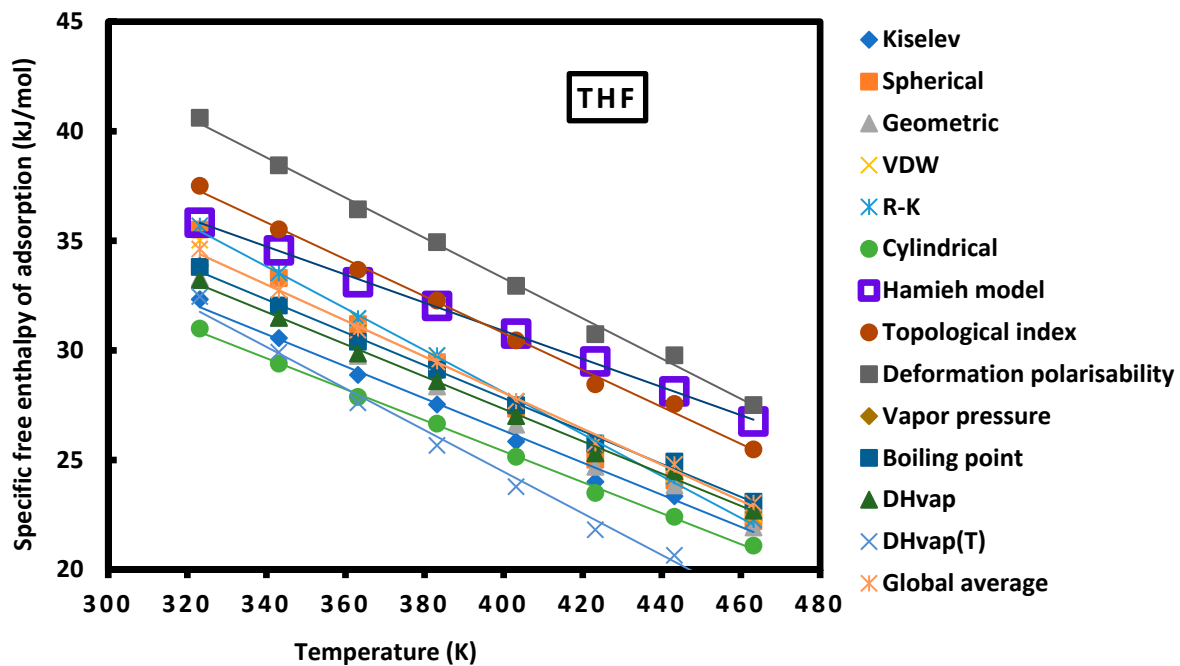
Figure 4d. Diethyl ether.
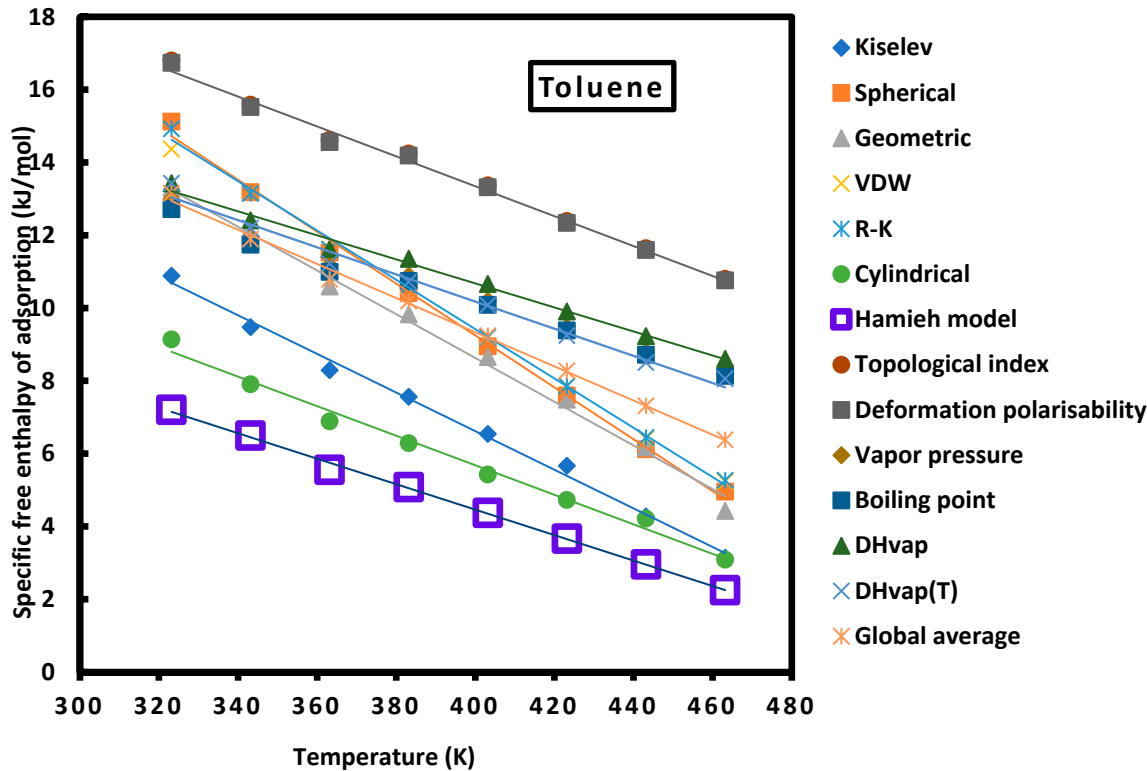

Figure 4e. THF.

Figure 4f. Toluene.

Figure 4. Variations of ΔG_a^{sp} as a function of the temperature for the various polar molecules adsorbed on alumina surface by using the different IGC models and methods.

Table 7. The linear equations of $-\Delta G_a^{sp}(T)$ (kJ/mol) of polar solvents adsorbed on alumina particles as a function of the temperature T (K) for all models and methods.

Model or method	Polar solvent	Equation $-\Delta G_a^{sp}(T)$ (kJ/mol)
Kiselev	CCl4	$-\Delta G_a^{sp}(T) = -0.015\ T + 9.951$
	CHCl3	$-\Delta G_a^{sp}(T) = -0.0950\ T + 66.196$
	CH2Cl2	$-\Delta G_a^{sp}(T) = -0.099\ T + 49.816$
	Diethyl ether	$-\Delta G_a^{sp}(T) = -0.104\ T + 76.237$
	THF	$-\Delta G_a^{sp}(T) = -0.073\ T + 55.663$
	Toluene	$-\Delta G_a^{sp}(T) = -0.053\ T + 27.836$
Spherical	CCl4	$-\Delta G_a^{sp}(T) = -0.022\ T + 12.846$
	CHCl3	$-\Delta G_a^{sp}(T) = -0.109\ T + 73.138$
	CH2Cl2	$-\Delta G_a^{sp}(T) = -0.115\ T + 58.418$
	Diethyl ether	$D-\Delta G_a^{sp}(T) = -0.090\ T + 71.08$
	THF	$-\Delta G_a^{sp}(T) = -0.095\ T + 65.952$
	Toluene	$-\Delta G_a^{sp}(T) = -0.071\ T + 37.748$
Geometric	CCl4	$-\Delta G_a^{sp}(T) = -0.038\ T + 22.904$
	CHCl3	$-\Delta G_a^{sp}(T) = -0.119\ T + 77.161$
	CH2Cl2	$-\Delta G_a^{sp}(T) = -0.121\ T + 60.18$
	Diethyl ether	$-\Delta G_a^{sp}(T) = -0.081\ T + 65.801$
	THF	$-\Delta G_a^{sp}(T) = -0.080\ T + 59.029$
	Toluene	$-\Delta G_a^{sp}(T) = -0.060\ T + 32.654$
Vand der Waals (VDW)	CCl4	$-\Delta G_a^{sp}(T) = -0.017\ T + 10.919$

	CHCl3	$-\Delta G_a^{sp}(T)$ = -0.101 T + 69.275
	CH2Cl2	$-\Delta G_a^{sp}(T)$ = -0.111 T + 56.128
	Diethyl ether	$-\Delta G_a^{sp}(T)$ = -0.085 T + 68.404
	THF	$-\Delta G_a^{sp}(T)$ = -0.091 T + 64.627
	Toluene	$-\Delta G_a^{sp}(T)$ = -0.066 T + 35.609
Redlich-Kwong (R-K)	CCl4	$-\Delta G_a^{sp}(T)$ = -0.021 T + 12.349
	CHCl3	$-\Delta G_a^{sp}(T)$ = -0.105 T + 70.824
	CH2Cl2	$-\Delta G_a^{sp}(T)$ = -0.113 T + 57.257
	Diethyl ether	$-\Delta G_a^{sp}(T)$ = -0.090 T + 70.46
	THF	$-\Delta G_a^{sp}(T)$ = -0.096 T + 66.356
	Toluene	$-\Delta G_a^{sp}(T)$ = -0.068 T + 36.511
Cylindrical	CCl4	$-\Delta G_a^{sp}(T)$ = -0.021 T + 12.489
	CHCl3	$-\Delta G_a^{sp}(T)$ = -0.135 T + 83.700
	CH2Cl2	$-\Delta G_a^{sp}(T)$ = -0.136 T + 65.871
	Diethyl ether	$-\Delta G_a^{sp}(T)$ = -0.088 T + 68.367
	THF	$-\Delta G_a^{sp}(T)$ = -0.071 T + 53.71
	Toluene	$-\Delta G_a^{sp}(T)$ = -0.041 T + 21.91
Hamieh model	CCl4	$-\Delta G_a^{sp}(T)$ = -0.006 T + 8.164
	CH2Cl2	$-\Delta G_a^{sp}(T)$ = -0.007 T + 29.475
	CHCl3	$-\Delta G_a^{sp}(T)$ = -0.099 T + 51.024
	Diethyl ether	$-\Delta G_a^{sp}(T)$ = -0.110 T + 76.509
	THF	$-\Delta G_a^{sp}(T)$ = -0.064 T + 56.551
	Toluene	$-\Delta G_a^{sp}(T)$ = -0.035 T + 18.456
Topological index	CCl4	$-\Delta G_a^{sp}(T)$ = -0.019 T + 19.115
	CH2Cl2	$-\Delta G_a^{sp}(T)$ = -0.111 T + 77.995
	CHCl3	$-\Delta G_a^{sp}(T)$ = -0.112 T + 58.858
	Diethyl ether	$-\Delta G_a^{sp}(T)$ = -0.088 T + 68.894
	THF	$-\Delta G_a^{sp}(T)$ = -0.084 T + 64.482
	Toluene	$-\Delta G_a^{sp}(T)$ = -0.041 T + 29.895
Deformation polarizability	CCl4	$-\Delta G_a^{sp}(T)$ = -0.022 T + 21.723
	CH2Cl2	$-\Delta G_a^{sp}(T)$ = -0.083 T + 57.101
	CHCl3	$-\Delta G_a^{sp}(T)$ = -0.100 T + 50.004
	Diethyl ether	$-\Delta G_a^{sp}(T)$ = -0.0922 T + 71.692
	THF	$-\Delta G_a^{sp}(T)$ = -0.092 T + 70.019
	Toluene	$-\Delta G_a^{sp}(T)$ = -0.041 T + 29.774
Vapor pressure	CCl4	$-\Delta G_a^{sp}(T)$ = 0.001 T + 4.7609
	CH2Cl2	$-\Delta G_a^{sp}(T)$ = -0.087 T + 61.958
	CHCl3	$-\Delta G_a^{sp}(T)$ = -0.091 T + 43.784
	Diethyl ether	$-\Delta G_a^{sp}(T)$ = -0.084 T + 66.903
	THF	$-\Delta G_a^{sp}(T)$ = -0.079 T + 59.071
	Toluene	$-\Delta G_a^{sp}(T)$ = -0.033 T + 23.369
Boiling point	CCl4	$-\Delta G_a^{sp}(T)$ = 0.002 T + 4.0546
	CH2Cl2	$-\Delta G_a^{sp}(T)$ = -0.091 T + 63.571
	CHCl3	$-\Delta G_a^{sp}(T)$ = -0.089 T + 42.024

	Diethyl ether	$-\Delta G_a^{sp}(T) = -0.087\ T + 68.002$
	THF	$-\Delta G_a^{sp}(T) = -0.075\ T + 57.849$
	Toluene	$-\Delta G_a^{sp}(T) = -0.031\ T + 22.645$
Enthalpy of vaporization DHvap(298K)	CCl4	$-\Delta G_a^{sp}(T) = 0.001\ T + 4.8875$
	CH2Cl2	$-\Delta G_a^{sp}(T) = -0.086\ T + 59.17$
	CHCl3	$-\Delta G_a^{sp}(T) = -0.091\ T + 43.106$
	Diethyl ether	$-\Delta G_a^{sp}(T) = -0.086\ T + 66.757$
	THF	$-\Delta G_a^{sp}(T) = -0.074\ T + 56.843$
	Toluene	$-\Delta G_a^{sp}(T) = -0.033\ T + 23.885$
Thermic enthalpy of vaporization DHvap(T)	CCl4	$-\Delta G_a^{sp}(T) = -0.018\ T + 10.116$
	CH2Cl2	$-\Delta G_a^{sp}(T) = -0.096\ T + 62.393$
	CHCl3	$-\Delta G_a^{sp}(T) = -0.115\ T + 49.546$
	Diethyl ether	$-\Delta G_a^{sp}(T) = -0.112\ T + 73.958$
	THF	$-\Delta G_a^{sp}(T) = -0.095\ T + 62.454$
	Toluene	$-\Delta G_a^{sp}(T) = -0.037\ T + 25.095$

3.2.2. Lewis's acid base parameters

From the equations $\Delta G_a^{sp}(T)$ on Tables 7, we deduced the values of $(-\Delta H_a^{sp})$ and $(-\Delta S_a^{sp})$ relative to the adsorption of CCl4, CH2Cl2, CHCl3, diethyl ether, THF and toluene on alumina particles by using the various molecular models and methods. The results were presented on Tables 8 and 9.

Table 8. Values of the specific enthalpy $(-\Delta H_a^{sp}\ in\ kJ\ mol^{-1})$ of the various polar solvents adsorbed on alumina by using the various molecular models, Hamieh model, topological index, deformation polarizability and vapor pressure methods compared to global average with the standard deviation and the error percentage.

Probes	CCl4	CHCl3	CH2Cl2	Diethyl ether	THF	Toluene
Kiselev	9.95	49.82	66.20	76.24	55.66	27.84
Spherical	12.85	58.42	73.14	71.08	65.95	37.75
Geometric	22.90	60.18	77.16	65.80	59.03	32.65
VDW	10.92	56.13	69.28	68.40	64.63	35.61
R-K	12.35	57.26	70.82	70.46	66.36	36.51
Cylindrical	12.49	65.87	83.70	68.37	53.71	21.91
Hamieh model	8.16	51.02	29.48	76.51	56.55	18.46
Topological index	19.12	58.86	78.00	68.89	64.48	29.90
Deformation polarizability	21.72	50.00	57.10	71.69	70.02	29.77
Vapor pressure	4.76	43.78	61.96	66.90	59.07	23.37
Boiling point	4.05	42.02	63.57	68.00	57.85	22.65
DHvap(298K)	4.89	43.11	59.17	66.76	56.84	23.89
DHvap(T)	10.12	49.55	62.39	73.96	62.45	25.10
Average values	11.87	52.77	65.54	70.24	60.97	28.11
Standard deviation	6.16	7.34	13.41	3.52	4.99	6.17
Error percentage	51.86	13.91	20.47	5.01	8.18	21.96

The calculations of the average, standard deviation and error percentage committed on the values of the specific enthalpy of adsorption on alumina reflect the dispersion of results obtained by the models and methods compared to the thermal model. One conluded here that the error with CCl4 is 51.86% followed by toluene (21.96%), CH2Cl2 (20.47%), CHCl3 (13.91%), THF (8.18%) and diethyl

ether (5.01%). The results on Table 8 showed that the IGC methods that match better the thermal models are the following: boiling point, vapor pressure and enthalpy of vaporization; followed by the other molecular models such as cylindrical and Kiselev models.

Table 9. Values of the specific entropy $(-\Delta S_a^{sp} \, in \, J \, K^{-1} mol^{-1})$ of the various polar solvents adsorbed on alumina by using the various molecular models, Hamieh model, topological index, deformation polarizability and vapor pressure methods compared to global average with the standard deviation and the error percentage.

Probes	CCl4	CHCl3	CH2Cl2	Diethyl ether	THF	Toluene
Kiselev	15.1	98.8	94.9	104.1	73.3	53
Spherical	22.2	114.5	108.8	90.2	95.2	71.3
Geometric	37.7	120.8	119.1	80.8	80.2	60.1
VDW	17	111.1	101.1	84.9	91.4	65.6
R-K	20.5	113.3	104.9	90.1	95.7	67.7
Cylindrical	20.5	133.5	134.7	87.7	70.8	40.6
Hamieh model	5.9	98.7	6.7	110.1	64.1	35
Topological index	18.5	112	111.2	88.4	84.2	41.2
Deformation polarizability	22	99.9	82.7	92.2	91.8	41.1
Vapor pressure	-0.6	91.2	86.6	83.7	78.8	32.8
Boiling point	-2.2	88.9	91.3	87	75.1	31.4
D$Hvap$(298K)	-1	90.5	85.5	85.5	73.8	33
D$Hvap$(T)	18.1	114.7	96.1	111.8	95	37.3
Average values	14.9	106.8	94.1	92.0	82.3	46.9
Standard deviation	11.48	13.31	30.08	10.07	10.68	14.61
Error percentage	77.02	12.46	31.97	10.94	12.98	31.15

For the specific entrop of adsorption (Table 9), the error percentage reaches 77.02 with CCl4, 31.97 with CH2Cl2 followed by THF (12.98%), CHCl3 (12.46%), THF (8.18%) and diethyl ether (5.01%). The closer methods to the thermal models are identical to those obtained with the specific enthalpy of adsorption proving the effect of the temperature on the surface area of organic molecules.

The acid base parameters of alumina were obtained from Tables 8 and 9 and allowed to plot Figures 5 and 6 representing the respective variations of $\left(\frac{-\Delta H_a^{sp}}{AN'}\right)$ and $\left(\frac{-\Delta S_a^{sp}}{AN'}\right)$ as a function of $\left(\frac{DN'}{AN'}\right)$. The excellent linearity obtained with the different models gave on Table 10 the values of Lewis enthalpic acid base constants K_A and K_D and Lewis entropic acid base constants ω_A and ω_D of alumina surface. The values of the acid base parameters obtained the thermal model are the following:

$$K_A = 0.624, \, K_D = 1.831 \text{ and } K_D/K_A = 2.93$$

$$\omega_A = 0.72, \, \omega_D = 2.79 \text{ and } \omega_D / \omega_A = 3.9$$

These results proved the amphoteric character of alumina surfaces with stronger Lewis's basicity about three times more important than the Lewis's acidity of alumina. The same tendency was observed with the entropic acid base parameters.
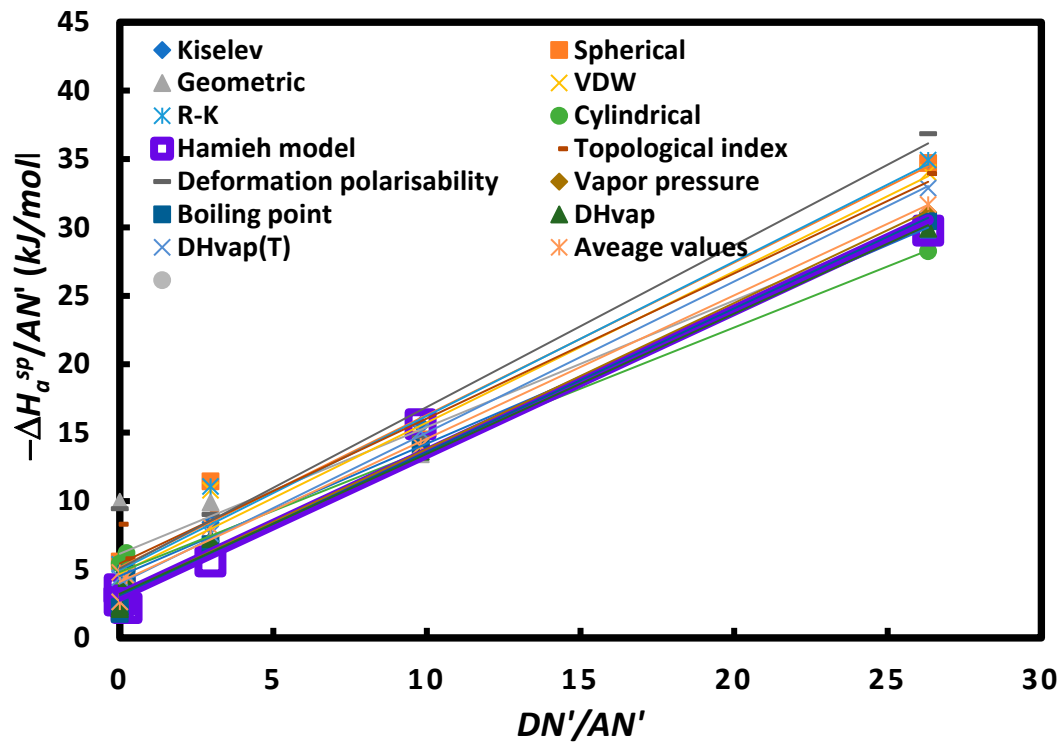
Figure 5. Variations of $\left(\frac{-\Delta H_a^{sp}}{AN'}\right)$ as a function of $\left(\frac{DN'}{AN'}\right)$ of different polar molecules adsorbed on alumina surface for different molecular models and IGC methods.
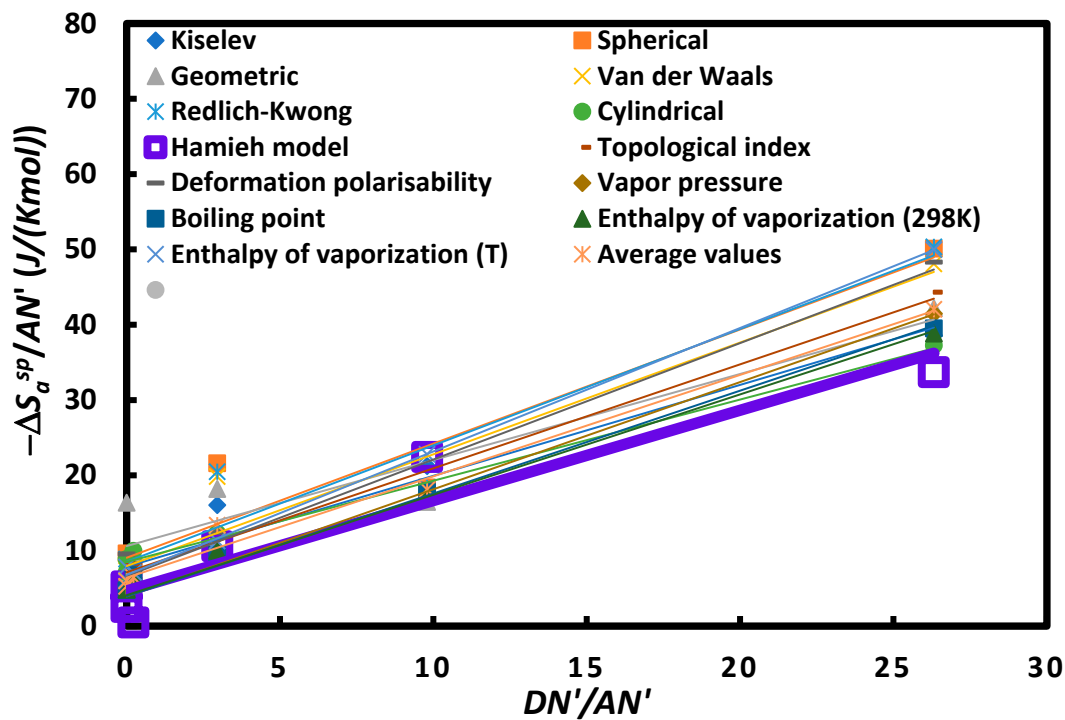

Figure 6. Variations of $\left(\frac{-\Delta S_a^{sp}}{AN'}\right)$ as a function of $\left(\frac{DN'}{AN'}\right)$ of different polar molecules adsorbed on alumina particles for different molecular models and IGC methods.

Table 10. Values of the enthalpic acid base constants K_A and K_D (unitless) and the entropic acid base constants ω_A and ω_D (unitless) of alumina surface and the acid base ratios for the different used molecular models and IGC methods.

Models and IGC methods	K_A	K_D	K_D/K_A	$10^3.\omega_A$	$10^3.\omega_D$	ω_D / ω_A

Kiselev	0.578	2.705	4.68	0.72	4.71	6.5
Spherical	0.665	3.093	4.65	0.91	5.42	6.0
Geometric	0.553	3.676	6.65	0.68	6.34	9.3
VDW	0.659	2.818	4.28	0.89	4.76	5.4
R-K	0.674	2.961	4.40	0.92	5.11	5.5
Cylindrical	0.534	2.879	5.39	0.64	5.09	7.9
Hamieh model	0.624	1.831	2.93	0.72	2.79	3.9
Topological index	0.633	3.250	5.13	0.82	4.27	5.2
Deformation polarizability	0.705	3.034	4.30	0.92	3.97	4.3
Vapor pressure	0.637	1.887	2.96	0.85	2.35	2.8
Boiling point	0.626	1.863	2.97	0.82	2.36	2.9
DHvap	0.612	1.928	3.15	0.80	2.46	3.1
DHvap(T)	0.659	2.376	3.60	0.98	4.07	4.2
Average values	0.628	2.639	4.20	0.82	4.13	5.0
Standard deviation	0.05	0.61		0.10	1.29	
Error percentage	7.78	22.96		12.79	31.34	

Table 10 showed that the best models or methods that gave results comparable to those obtained by the thermal model are the following: boiling point, vapor pressure and enthalpy of vaporization methods proving the important effect of the temperature on the surface areas adsorbed on alumina particles.

4. Discussion

Since 1982, scientists were interested to the determination of physicochemical properties of materials by using inverse gas chromatography at infinite dilution. Saint-Flour and Papirer [12,13] have first tried to separate the two dispersive and polar contributions of the Gibbs free energy of adsorption of polar solvents on solid substrates by using the notion of vapor pressure of organic molecules. Schultz et al [73], Donnet et al. [80], Brendlé and Papirer [2] and other scientists [10,14,20,23,33,36,59] were also interested to the determination of specific and dispersive properties of materials. There was no universal method or model to be used in IGC at infinite dilution for an accurate characterization of solid particles. Even Dorris-Gray relation [71] cannot give a precise value of the dispersive component of the solid surface of solid materials. Hamieh et al. [35,77,78,81] have nevertheless succeeded in carrying out a very precise determination of the second-order temperatures (such as the glass transition) of polymers such as poly (methyl methacrylate) or pol (a-n-alkyl) methacrylate in bulk phase or in adsorbed state. The serious difficulty faced by researchers during 40 years was the problem of the diversity of methods and models used to determine the surface properties of a solid material such as the dispersive free surface energy, the specific free energy and the Lewis's acid-base constants without obtaining the same results. Indeed, we proved in several previous studies that the various models and methods of IGC technique did not give the same results. On the contrary, the methods used gave results completely different from each other. The error percentage sometimes exceeds 100% from one method to another. Our previous works highlighted the important effect of the temperature on the surface area of organic solvents. We failed the methods proposed by Dorris-Gray [71] and Schultz et al. [73] that supposed a constant value of the surface area of organic molecules and we proposed various relations of the surface area of probes depending on the temperature and corrected the values of the dispersive surface energy and polar properties of materials. Our new methodology was applied to the alumina particles and determined with an excellent accuracy the surface physicochemical properties of alumina. The thermal model [69] has to be applied in the future for a good characterization of solid surfaces.

On the other hand, we observed similar results between the thermal model [69] and those given by equations (27) and (28) by using the values of the standard enthalpy ($-\Delta H_a^0$) and entropy ($-\Delta S_a^0$) of adsorption of polar molecules on alumina surfaces. The last way can resolve some difficulties

related to the choose of the best model for more accurate results of the surface thermodynamic properties of materials.

5. Conclusions

The surface thermodynamic properties such as the London dispersive component of the surface energy, the Gibbs free energy of adsorption, the specific interactions and the Lewis's acid base parameters of alumina particles were determined by using the inverse gas chromatography technique at infinite dilution an applying 15 molecular models and chromatographic methods.

The determination of the London dispersive surface energy of alumina by using the various molecular models showed that Dorris-Gray formula [71] and Schultz et al. method [73] cannot be used for an accurate determination of γ_s^d of solid alumina. We corrected the calculation of γ_s^d (T) by using the new thermal model that took into account the change of the surface areas $a(T)$ of organic molecules as a function of the temperature. The following relation was therefore obtained:

$$\gamma_s^d(T) = 0.480T + 233.9$$

with a dispersive surface entropy equal to $\varepsilon_s^d = -0.480\ mJ\ m^{-2}K^{-1}$ and the maximum of temperature, characteristic of alumina, equal to $T_{Max} = 487.21K$.

The specific Gibbs free energy was obtained by the different molecular models and methods. All methods were proved to be inaccurate except that of the thermal model. However, the methods based on the effect of the temperature on the thermodynamic parameters such as the vapor pressure, the boiling point temperature and the standard enthalpy of vaporization gave results closer to those obtained by Hamieh thermal model [69]. We gave below the variations of the Specific Gibbs free energy $\Delta G_a^{sp}(T)$ of polar molecules adsorbed on alumina surfaces as a function of the temperature with the values of the specific enthalpy and entropy of adsorption.

Polar molecule	$\Delta G_a^{sp}(T)$(kJ/mol)	ΔH_a^{sp} (kJ/mol)	$\Delta S_a^{sp}(JK^{-1}mol^{-1})$
CCl4	$-\Delta G_a^{sp}$(T) = -0.021 T + 12.489	12.489	21
CH2Cl2	$-\Delta G_a^{sp}$(T) = -0.135 T + 83.700	83.700	135
CHCl3	$-\Delta G_a^{sp}$(T) = -0.136 T + 65.871	65.871	136
Diethyl ether	$-\Delta G_a^{sp}$(T) = -0.088 T + 68.367	68.367	88
THF	$-\Delta G_a^{sp}$(T) = -0.071 T + 53.71	53.71	71
Toluene	$-\Delta G_a^{sp}$(T) = -0.041 T + 21.91	21.91	41

These results clearly showed the strong Lewis basicity of alumina proved by the strong interactions between the more acidic solvent (CH2Cl2) with ΔH_a^{sp}= 83.700 kJ/mol and also an important amphoteric character.

The use of the thermal model led to the following Lewis acid base parameters:

$$K_A = 0.624, K_D = 1.831 \text{ and } K_D/K_A = 2.93$$

$$\omega_A = 0.72, \omega_D = 2.79 \text{ and } \omega_D / \omega_A = 3.9$$

Thus, showing that the alumina surface is about three times more basic than acidic. The same tendency was observed with the entropic acid base parameters. Comparable values of the acid base parameters of alumina were obtained by using the methods of vapor pressure, boiling point or the standard enthalpy of vaporization.

The new methodology proposed in this study will therefore allow to obtain an accurate determination of the London dispersive surface energy, the Gibbs free energy, the specific enthalpy and entropy of adsorption of polar molecules on the solid surfaces as well as the Lewis acid base parameters of solid substrates.

References

1. Pyda M.; Guiochon, G. Surface properties of silica-based adsorbents measured by inverse gas–solid chromatography at finite concentration, *Langmuir* **1997**, 13, 1020–1025.
2. Brendlé, E.; Papirer, E. A new topological index for molecular probes used in inverse gas chromatography for the surface nanorugosity evaluation, 2. Application for the Evaluation of the Solid Surface Specific Interaction Potential, *J. Colloid Interface Sci.* **1997**, 194, 217–224.
3. Thielmann, F.; Baumgarten, E. Characterization of Microporous Aluminas by Inverse Gas Chromatography, *J. Colloid Interface Sci.* **2000**, 229(2), 418-422, https://doi.org/10.1006/jcis.2000.6958.
4. Onjia, A. E.; Milonjić, S. K.; Todorović, M.; Loos-Neskovic, C.; Fedoroff, M. ; Jones, D. J. An inverse gas chromatography study of the adsorption of organics on nickel- and copper-hexacyanoferrates at zero surface coverage, *J. Colloid Interface Sci.* **2002,** 251, 10-17, https://doi.org/10.1006/jcis.2002.8372.
5. Conder, J.R.; Locke, D.C.; Purnell, J.H. Concurrent solution and adsorption phenomena in chromatography. *I. J. Phys. Chem.* **1969,** 73, 700-8. https://doi.org/10.1021/j100723a035.
6. Conder, J.R.; Purnell, J.H. Gas chromatography at finite concentrations. Part 2.—A generalized retention theory. *Trans Faraday Soc.* **1968,** 64, 3100–11.
7. Conder, J.R.; Purnell, J.H. Gas chromatography at finite concentrations. Part 3.—Theory of frontal and elution techniques of thermodynamic measurement. *Trans Faraday Soc.* **1969,** 65, 824-38. https://doi.org/10.1039/TF9696500824
8. Conder, J.R.; Purnell, J.H. Gas chromatography at finite concentrations. Part 4.—Experimental evaluation ofmethods for thermodynamic study of solutions. *Trans Faraday Soc.* **1969,** 65, 839-48. https://doi.org/10.1039/TF9696500839
9. Conder, J.R.; Purnell, J.H. Gas chromatography at finite concentrations. Part 1.—Effect of gas imperfection on calculation of the activity coefficient in solution from experimental data. *Trans Faraday Soc.* **1968,** 64, 1505-12. https://doi.org/10.1039/TF9686401505.
10. Papirer, E.; Balard H.; Rahmani Y.; Legrand, A.; Facchini, L.; Hommel, H. Characterization by inverse gas chromatography of the surface properties of silicas modified by poly (ethylene glycols) and their models (oligomers, diols). *Chromatographia* **1987**, 23, 639-47. https://doi.org/10.1007/BF02311491.
11. Vidal, A.; Papirer, E.; Jiao, W.M.; Donnet, J.B. Modification of silica surfaces by grafting of alkyl chains. I-Characterization of silica surfaces by inverse gas–solid chromatography at zero surface coverage. *Chromatographia* **1987,** 23, 121-8. https://doi.org/10.1007/BF02312887
12. Saint Flour, C., Papirer, E. Gas-solid chromatography. A method of measuring surface free energy characteristics of short glass fibers. 1. Through adsorption isotherms. *Ind Eng Chem Prod Res Dev.* **1982,** 21, 337-341. https://doi.org/10.1021/i300006a029.
13. Saint Flour, C., Papirer, E. Gas-solid chromatography: method of measuring surface free energy characteristics of short fibers. 2. Through retention volumes measured near zero surface coverage. *Ind Eng Chem Prod Res Dev.* **1982,** 21, 666-669. https://doi.org/10.1021/i300008a031.
14. Papirer, E.; Balard, H.; Vidal, A. Inverse gas chromatography: a valuable method for the surface characterization of fillers for polymers (glass fibres and silicas). *Eur Polym J.* **1988**, 24, 783-90. https://doi.org/10.1016/0014-3057(88)90015-8
15. Voelkel, A. Inverse gas chromatography: characterization of polymers, fibers, modified silicas, and surfactants. *Crit Rev Anal Chem.* **1991**, 22, 411-39. https://doi.org/10.1080/10408349108051641.
16. Schuster, R.H.; Gräter, H.; Cantow, H.J. (1984) Thermodynamic studies on polystyrene-solvent systems by gas chromatography. *Macromolecules* **1984,** 17, 619-25. https://doi.org/10.1021/ma00134a018.
17. Öner, M.; Dincer, S. Thermophysical properties of polymer-probe pairs by gas chromatography. *Polymer* **1987,** 28, 279-82. https://doi.org/10.1016/0032-3861(87)90417-4.
18. Guillet, J. E.; Romansky, M.; Price, G.J.; Van der Mark, R. Studies of polymer structure and interactions by automated inverse gas chromatography. Inverse gas chromatography. 1989, Washington, DC: Characterization of Polymers and Other Materials, American Chemical Society 20–32. *Eng. Asp.,* **2002,** 206, 547-554.
19. Katsanos, N. A.; Gavril, D.; Kapolos, J.; Karaiskakis, G. Surface energy of solid catalysts measured by inverse gas chromatography, *J. Colloid Interface Sci.,* 270(2) (2004) 455-461. https://doi.org/10.1016/j.jcis.2003.07.037.
20. Balard, H.; Brendlé, E.; Papirer, E. Determination of the acid–base properties of solid surfaces using inverse gas chromatography: advantages and limitations. In: Mittal, K.L., Editor. Acid–Base Interactions, Relevance to Adhesion Science and Technology. Vol. 2: CRC Press; 2000. p. 299–316.
21. Kemball, C.; Rideal, E.K. The adsorption of vapours on mercury I) Non –polar substances, *Proceedings of the Royal Society of London. Series A* **1946,** 187, 53-73.
22. Onjia, A. E.; Milonjić, S. K.; Todorović, M.; Loos-Neskovic, C.; Fedoroff, M.; Jones, D. J. An inverse *gas chromatography* study of the adsorption of organics on nickel- and copper-hexacyanoferrates at zero surface coverage, *J. Colloid Interface Sci.* **2002,** 251, 10-17, https://doi.org/10.1006/jcis.2002.8372.
23. Donnet, J.-B.; Ridaoui, H.; Balard, H.; Barthel, H.; Gottschalk-Gaudig, T. Evolution of the surface polar character of pyrogenic silicas, with their grafting ratios by dimethylchlorosilane, studied by microcalorimetry, *J. Colloid Interface Sci.* **2008,** 325, 101-106. https://doi.org/10.1016/j.jcis.2008.05.025.

24. Papirer, E.; Brendlé, E.; Balard, H.; Dentzer, J. Variation of the surface properties of nickel oxide upon heat treatment evidenced by temperature programmed desorption and inverse gas chromatography studies. *J. Mater. Sci.* **2000,** 35, 3573-3577.

25. Rodriguez, M.; Rubio, J.; Rubio, F.; Liso, M.; Oteo, J. Application of inverse gas chromatography to the study of the surface properties of slates. *Clays Clay Miner.* **1997,** 45, 670-680.

26. Przybyszewska, M.; Krzywania, A.; Zaborski, M.; Szynkowska, M.I. Surface properties of zinc oxide nano-particles studied by inverse gas chromatography, *J. Chromatogr. A* **2009,** 1216, 5284-5291.

27. Ali, S.; Heng, J.; Nikolaev, A.; Waters, K. Introducing inverse gas chromatography as a method of determining the surface heterogeneity of minerals for flotation, *Powder Technol.* **2013**, 249, 373-377.

28. Shi, X.; Bertóti, I.; Pukánszky, B.; Rosa, R.; Lazzeri, A. Structure and surface coverage of water-based stearate coatings on calcium carbonate nanoparticles, *J. Colloid Interface Sci.* **2011,** 362, 67-73, https://doi.org/10.1016/j.jcis.2011.06.025.

29. Mohammadi-Jam, S.; Burnett, D.J., Waters, K.E.; Surface energy of minerals —Applications to flotation. *Miner. Eng.* **2014**, 66 to 68, 112-118 http://dx.doi.org/10.1016/j.mineng.2014.05.002.

30. Daoui, H.; Boutoumi, H.; Bouhamidi, Y.; Boucherit, A.; Zouikri, M. Characterization of an Algerian diatomite by inverse gas chromatography: Specific and non-specific contribution and Lewis acid–base parameters, *International Journal of Polymer Analysis and Characterization* **2018,** 23(5), 463-473, https://doi.org/10.1080/1023666X.2018.1478247.

31. Shui, M.; Reng, Y.; Pu, B.; Li, J. Variation of surface characteristics of silica-coated calcium carbonate, *J. Colloid Interface Sci.* **2004,** 273, 205-210, https://doi.org/10.1016/j.jcis.2004.01.018.

32. Rückriem, M.; Inayat, A.; Enke, D.; Gläser, R.; Einicke, W-D.; Rockmann, R. Inverse gas chromatography for determining the dispersive surface energy of porous silica. *Colloids Surf A Physicochem. Eng. Asp.* **2010,** 357, 21-26.

33. Donnet, J.-B.; Balard, H.; Nedjari, N.; Hamdi, B.; Barthel, H.; Gottschalk-Gaudig, T. Influence of specific surface area of pyrogenic silicas on their heat of immersion in water and on their surface properties assessed using inverse gas chromatography, *J. Colloid Interface Sci.* **2008,** 328, 15-9. https://doi.org/10.1016/j.jcis.2008.09.005.

34. Bandosz, T.J.; Putyera, K.; Jagiełło, J.; Schwarz, J.A. Application of inverse gas chromatography to the study of the surface properties of modified layered minerals, *Microporous Mater.* **1993**, 1 (1993) 73–79.

35. Hamieh, T.; Rezzaki, M.; Grohens, Y.; Schultz, J. Glass transition of adsorbed stereoregular PMMA by inverse gas chromatography at infinite dilution, *J. Chim. Phys.*, **1998,** 95, 1964-1990.

36. Boudriche, L.; Chamayou, A.; Calvet, R.; Hamdi, B.; Balard, H. Influence of different dry milling processes on the properties of an attapulgite clay, contribution of inverse gas chromatography. *Powder Technol.* **2014**, 254, 352-363.

37. Bauer, F.; Meyer, R.; Czihal, S.; Bertmer, M.; Decker, U.; Naumov, S.; Uhlig, H.; Steinhart, M.; Enke, D. Functionalization of porous siliceous materials, Part 2: Surface characterization by inverse gas chromatography, *J. Chromatogr. A* **2019**, 1603, 297-310, https://doi.org/10.1016/j.chroma.2019.06.031.

38. Yao, Z.; Wu, D.; Heng, J.Y.Y.; Lanceros-Mendez, S.; Hadjittofis, E.; Su, W.; Tang, J.; Zhao, H.; Wu W.; et al. Comparative study of surface properties determination of colored pearl-oyster-shell-derived filler using inverse gas chromatography method and contact angle measurements, *International Journal of Adhesion and Adhesives*, **2017,** 78, 55-59, http://dx.doi.org/10.1016/j.ijadhadh.2017.06.018

39. Rueckriem, M.; Hahn, T.; Enke, D. Inverse gas chromatographic studies on porous glass, *Opt. Appl.* **2012,** 42, 295-306.

40. Batko, K.; Voelkel, A. Inverse gas chromatography as a tool for investigation of nanomaterials, *J. Colloid Interface Sci.* **2007,** 315(2), 768-771, https://doi.org/10.1016/j.jcis.2007.07.028.

41. Zhang, X.; Yang, D.; Xu, P.; Wang, C.; Du, Q. Characterizing the surface properties of carbon nanotubes by inverse gas chromatography, *J. Mater. Sci.* **2007**, 42, 7069-7075.

42. Demertzis, P.; Riganakos, K.; Kontominas, M. Water sorption isotherms of crystalline raffinose by inverse gas chromatography. *Int. J. Food Sci. Technol.* **1989**, 24, 629-636.

43. Helen, H.; Gilbert, S. Moisture sorption of dry bakery products by inverse gas chromatography. *J. Food Sci.* **1985**, 50, 454-458.

44. Menzel, R.; Bismarck, A.; Shaffer, M.S. Deconvolution of the structural and chemical surface properties of carbon nanotubes by inverse gas chromatography, *Carbon*, **2012**, 50, 3416-3421.

45. Menzel, R.; Lee, A.; Bismarck, A.; Shaffer, M.S. Inverse gas chromatography of as received and modified carbon nanotubes, *Langmuir*, **2009**, 25, 8340-8348.

46. Shih, Y.-H.; Li, M.-S. Adsorption of selected volatile organic vapors on multiwall carbon nanotubes, *J. Hazard. Mater.* **2008**, 154, 21-8.

47. Gamble, J.F.; Davé, R.N.; Kiang, S.; Leane, M.M.; Tobyn, M.; Wang, S.S.S. Investigating the applicability of inverse gas chromatography to binary powdered systems: an application of surface heterogeneity profiles to understanding preferential probe–surface interactions, *Int. J. Pharm.* **2013**, 445, 39-46.

48. Jones, M.D.; Young, P.; Traini, D. The use of inverse gas chromatography for the study of lactose and pharmaceutical materials used in dry powder inhalers, *Adv. Drug. Deliv. Rev.* **2012**, 64, 285-293.

49. Grimsey, I.M.; Feeley, J.C.; York, P. Analysis of the surface energy of pharmaceutical powders by inverse gas chromatography, *J. Pharm. Sci.*, **2002**, 91, 571-583.

50. Guo, Y.; Shalaev, E.; Smith, S. Solid-state analysis and amorphous dispersions in assessing the physical stability of pharmaceutical formulations, *Trends Anal. Chem.*, **2013**, 49, 137-144.

51. Chamarthy, S.P. The different roles of surface and bulk effects on the functionality of pharmaceutical materials, *Thesis*, **2007**, Purdue University, West Lafayette, Indiana. https://www.proquest.com/docview/304841067

52. Zhang, D.; Flory, J.; Panmai, S.; Batra, U.; Kaufman, M. Wettability of pharmaceutical solids: its measurement and influence on wet granulation, *Colloids Surf. A Physicochem. Eng. Asp.* **2002**, 206, 547-554.

53. Das, S.C.; Stewart, P.J. Characterising surface energy of pharmaceutical powders by inverse gas chromatography at finite dilution, *J. Pharm. Pharmacol.*, **2012**, 64, 1337-1348.

54. Telko, M.J.; Hickey, A.J. Critical assessment of inverse gas chromatography as means of assessing surface free energy and acid–base interaction of pharmaceutical powders, *J. Pharm. Sci.* **2007**, 96, 2647-2654.

55. Autie-Pérez, M.M.; Infantes-Molina, A.; Cecilia, J.A.; Labadie-Suarez, J. M.; Fernández-Echevarría, H.; Santamaría-González, J.; Rodríguez-Castellón, E. Light n-paraffins separation by inverse gas chromatography with Cuban volcanic glass, *Braz. J. Chem. Eng.* **2019**, 36 (1), 531 - 539. http://dx.doi.org/10.1590/0104-6632.20190361s20170470.

56. Contreras-Larios, J.L.; Infantes-Molina, A.; Negrete-Melo, L.A.; Labadie-Suarez, J. M.; Yee-Madeira, H.T.; Autie-Pérez, M.A.; Rodríguez-Castellón, E. Separation of N–C_5H_{12}–C_9H_{20} Paraffins Using Boehmite by Inverse Gas Chromatography, *Appl. Sci.* **2019,** 9 (9), 1810. https://doi.org/10.3390/app9091810.

57. Conder, J.R.; Young, C.L. Physical measurements by gas chromatography. 1979, Eds: Wiley J and Sons, New York.

58. Donnet, J.B.; Qin, R.Y. Empirical estimation of surface energies of polymers and their temperature dependence, *J. Colloid Interface Sci.* **1992**, 154(2), 434-443.

59. Chehimi, M.M.; Pigois-Landureau, E. Determination of acid–base properties of solid materials by inverse gas chromatography at infinite dilution. A novel empirical method based on the dispersive contribution to the heat of vaporization of probes, *J. Mater. Chem.* 1994, 4, 741-745.

60. Shi, B. Problem in the molecular area of polar probe molecules used in inverse gas chromatography, *J. Chromatogr. A*. **2019,** 1601, 385-387, https://doi.org/10.1016/j.chroma.2019.05.027.

61. Sun, C.; Berg, J. C. The effective surface energy of heterogeneous solids measured by inverse gas chromatography at infinite dilution, *J. Colloid Interface Sci.*, **2003**, 260(2), 443-448, https://doi.org/10.1016/S0021-9797(02)00238-2.

62. Gutmann, V. The Donor-acceptor Approach to Molecular Interactions, 1978, Plenum. New York.

63. Papirer, E.; Brendlé, E.; Balard, H.; Ozil, F. IGC determination of surface properties of fullerenes: comparison with other carbon materials.; *Carbon*, **1999**; 37:1265-1274.

64. Hamieh, T.; Fadlallah, M.-B.; Schultz J. New approach to characterise physicochemical properties of solid substrates by inverse gas chromatography at infinite dilution. III. Determination of the acid-base properties of some solid substrates (polymers, oxides and carbon fibres): a new model. *J. Chromatogr. A.*, **2002**, 969(1-2), 37-47, doi: 10.1016/S0021-9673(02)00358-8.

65. Hoss, D.J.; Knepper, R.; Hotchkiss, P.J.; Tappan, A.S.; Beaudoin, S.P. An evaluation of complementary approaches to elucidate fundamental interfacial phenomena driving adhesion of energetic materials, *J. Colloid Interface Sci.* **2016,** 4731, 28-33, https://doi.org/10.1016/j.jcis.2016.03.024.

66. Sun, C.; Berg, J. C. The effective surface energy of heterogeneous solids measured by inverse gas chromatography at infinite dilution, *J. Colloid Interface Sci.* **2003**, 260(2), 443-448, https://doi.org/10.1016/S0021-9797(02)00238-2.

67. Margariti, S.; Bassiotis, I.; Roubani-Kalantzopoulou, F. Physicochemical characterization of interfaces, *J. Colloid Interface Sci.* **2004,** 274(2), 413-420, https://doi.org/10.1016/j.jcis.2004.02.025.

68. Fekete, E.; Móczó, J.; Pukánszky, B. Determination of the surface characteristics of particulate fillers by inverse gas chromatography at infinite dilution: a critical approach, *J. Colloid Interface Sci.*, **2004**, 269 (1), 143-152.

69. Hamieh, T. Study of the temperature effect on the surface area of model organic molecules, the dispersive surface energy and the surface properties of solids by inverse gas chromatography, *J. Chromatogr. A*, **2020**, 1627, 461372.

70. Sawyer, D.T.; Brookman, D.J. Thermodynamically based gas chromatographic retention index for organic molecules using salt-modified aluminas and porous silica beads, *Anal. Chem.* **1968**, 40, 1847-1850. https://doi.org/10.1021/ac60268a015.

71. Dorris, G.M.; Gray, D.G. Adsorption of normal-alkanes at zero surface coverage on cellulose paper and wood fibers. *Journal of Colloid and Interface Science*. **1980**, 77,353-362.

72. Fowkes, F.M. in: Surface and interfacial aspects of biomedical polymers, **1985**, Vol. I, pp. 337-372, Ed: Andrade, J. D., Plenum Press, New York.

73. Schultz, J.; Lavielle, L.; Martin, C. The role of the interface in carbon fibre-epoxy composites. J. Adhes. **1987**, 23, 45-60.

23

74. Hamieh, T.; Schultz J. Etude par chromatographie gazeuse inverse de l'influence de la température sur l'aire de molécules adsorbées, *J. Chim. Phys.* **1996**, 93, 1292-1331.

75. Hamieh, T.; Schultz J. Study of the adsorption of n-alkanes on polyethylene surface - State equations, molecule areas and covered surface fraction, *Comptes Rendus de l'Académie des Sciences, Série IIb* **1996,** 323 (4), 281-289,

76. Hamieh, T.; Schultz J. A new method of calculation of polar molecule area adsorbed on MgO and ZnO by inverse gas chromatography, *Comptes Rendus de l'Académie des Sciences, Série IIb.* **1996**, 322 (8), 627-633.

77. Hamieh, T.; Rezzaki M.; Schultz J. Study of the second order transitions and acid-base properties of polymers adsorbed on oxides, by using inverse gas chromatography at infinite dilution, I Theory and Methods, *J. Colloid Interface Sci.*, **2001**, 233 (2), 339-342. https://doi.org/10.1006/jcis.2000.7267.

78. Hamieh, T.; Rezzaki M.; Schultz J. Study of the transition temperatures and acid-base properties of poly (methyl methacrylate) adsorbed on alumina and silica, by using inverse gas chromatography technique. Colloids and Surfaces A: Physicochemical and Engineering Aspects. **2001**, 189(1-3), 279-291. https://doi.org/10.1016/S0927-7757(01)00597-0

79. Hamieh, T.; Schultz J. New approach to characterise physicochemical properties of solid substrates by inverse gas chromatography at infinite dilution. *Journal of Chromatography A.* **2002**, 969(1-2), 17-47. https://doi.org/10.1016/S0021-9673(02)00368-0.

80. Donnet, J.B.; Park, S.; Balard, H. Evaluation of specific interactions of solid surfaces by inverse gas chromatography, *Chromatographia*. **1991**, 31:434-440.

81. Hamieh, T.; Rezzaki M.; Schultz J. Study of the second order transitions and acid-base properties of polymers adsorbed on oxides, by using inverse gas chromatography at infinite dilution, II Experimental results, *J. Colloid Interface Sci.*, **2001**, 233 (2), 343-347. https://doi.org/10.1006/jcis.2000.7271.

82. Riddle, F. L.; Fowkes, F. M. Spectral shifts in acid-base chemistry. Van der Waals contributions to acceptor numbers, Spectral shifts in acid-base chemistry. 1. van der Waals contributions to acceptor numbers. **1990**, *J. Am. Chem. Soc.*, 112 (9), 3259-3264. https://doi.org/10.1021/ja00165a001.

83. Hamieh, T. New methodology to study the dispersive component of the surface energy and acid–base properties of silica particles by inverse gas chromatography at infinite dilution, *Journal of Chromatographic Science* **2022**, 60 (2), 126-142, https://doi.org/10.1093/chromsci/bmab066.